JOURNAL OF MATERIALS SCIENCE 26 (1991) 917–924

Discontinuous crack growth in polyethylene under a constant load

X. LU, R. QIAN, N. BROWN
Department of Materials Science and Engineering, University of Pennsylvania, Philadelphia, Pennsylvania 19104-6272, USA

The kinetics of slow crack growth were measured in a polyethylene copolymer in a notched tensile specimen under constant load. The microscopic changes in the crack morphology were linked to the crack opening displacement and to the crack advance. The jump distance during the discontinuous crack growth decreased as the applied stress decreased. The jump distance decreased as the temperature decreased because the yield point was increasing. These observations are explainable by the Dugdale theory. The initiation time for fracture depends on the rate of disentanglement of the fibrils in the craze and occurs in the fibrils adjacent to a tough skin at the base of the craze. The crack grows until it meets fibrils whose strength matches the value of the stress intensity at which point the crack is arrested. Re-initiation of fracture occurs when the fibrils at the root of the crack have been sufficiently weakened by the process of disentanglement. Thus, the overall kinetics depend on (1) the rate of disentanglement of the fibrils, (2) the gradient in the fibrilla strength between the base and the tip of the craze, (3) the value of the stress intensity, and (4) the yield point of the matrix.

1. Introduction

When polyethylene gas pipes were first introduced in the USA about 1965, the time-dependent fracture under a constant stress displayed markings which indicated discontinuous crack growth. These discontinuities were reminiscent of the discontinuous crack growth that is often observed in the fatigue of polymers as shown by Hertzberg and Manson [1]. A clear presentation of how the discontinuous crack growth occurs in polymers under a constant stress has never been presented from the microscopic and kinetic viewpoint. The discontinuities or arrest lines were noted by Chan and Williams [2] and referred to as a "slip–stick mechanism" which they associated with crack blunting. Lustiger and Corneliussen [3] and Brown and Lu [4] also observed arrest lines in polyethylene without giving clear explanation of how they formed. Heston [5] presented a theoretical model for discontinuous crack growth based on the nucleation and growth of voids at the root of a crack in a crystalline solid.

In this paper a complete picture is given for the process of discontinuous crack growth in a polyethylene as viewed by the optical and scanning electron microscopes. The kinetics of the process were observed as a function of stress and temperature. The quantitative measures of the crack advance were linked to the detailed microscopic observations. The Dugdale theory, in conjunction with the kinetics of disentanglement and the structure of the craze, provides the basis for understanding the process of discontinuous slow crack growth.

2. Experimental procedure

Test specimens were cut from 4 in. (~ 10.16 cm) MDPE gas pipe, extruded in 1987. The thickness of the pipe wall is 10.5 mm. The average density of the pipe is 0.9413 g cm^{-3}. It is an ethylene–octene copolymer with 4.5 hexyl branches per 1000 carbons.

The geometry of the single-edge notched tension specimen is shown in Fig. 1. The length direction of the specimen is the axial direction of the pipe. The notch was made by razor blade at a speed of 50 μm min^{-1} along the inside surface of the pipe. The 3.5 mm depth of the notch was measured from the lowest point of the curved inside surface of the pipe. There are two 1 mm side grooves. The single-edge notched tensile specimen in Fig. 1 was designed to fracture under plane strain conditions. Fig. 2 is a schematic representation of the experimental apparatus. A microscope with a filar eyepiece was used to measure the notch opening at the specimen surface, AA, at the notch tip, CC, and at the thickness of the base of the damage zone, BB. CC is at the depth of insertion of the razor blade. The magnification of the microscope is × 20. The tests were conducted between 42 and 80 °C with the temperature being held constant within ± 0.5 °C.

A micrometer was used to measure the forward movement of the object lens of the microscope in order to measure the crack advance, Δa, by first focusing on the original notch tip and then on the root of the advancing crack. The morphology of damage zone at the notch tip was observed from three directions using the optical and electron microscope. The front view was obtained through the eyepiece of the optical microscope that was used to measure the COD and crack advance. The side view of the damage zone was obtained by slicing the specimen along an interior plane and then viewing a thin slice with the optical

0022–2461/90 $03.00 + .12

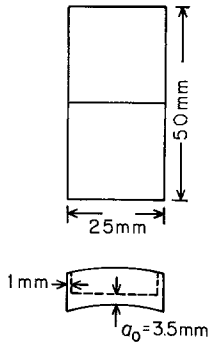

Figure 1 Specimen geometry.

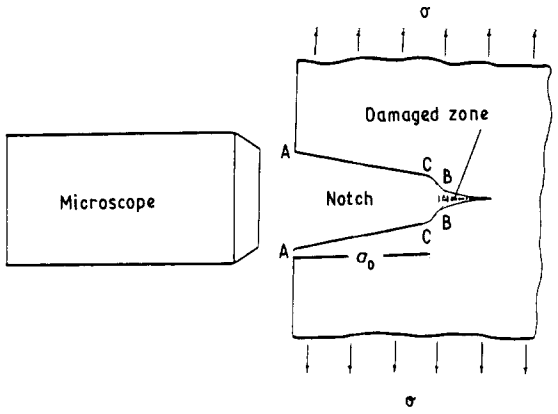

Figure 2 Experimental set-up.

microscope. The top view of the fractured surface was observed with an SEM.

3. Experimental results

3.1. Kinetics of discontinuous crack growth

The phenomenon of discontinuous crack growth is shown in Fig. 3 in which the notch opening, CC, and the crack advance, Δa, were measured simultaneously as a function of loading time. Both notch opening, CC, and crack advance, Δa, increased stepwise. There were four intervals during which the notch opened very slowly. These time intervals were 0 to 300, 350 to 475, 525 to 650, and 675 to 900 min. Following each of these slow intervals there was a jump in the notch opening. The average rate of crack opening displacement was about 1 $\mu m\,min^{-1}$ in the slow interval and about 12 $\mu m\,min^{-1}$ in the jump interval. The increment of CC in each jump is about 600 μm. It is important to note that the jump in CC happened during the same time interval as when the crack advanced rapidly.

3.2. Morphology

The morphological changes that are observed by looking directly into the notch are shown in Fig. 4. The morphological changes that are observed by viewing the damage process from a side view are shown in Fig. 5. Fig. 5 was obtained by slicing a series of specimens loaded at the same stress, but after various time intervals. Fig. 4 represents the changes in morphology with time on the same specimen. The

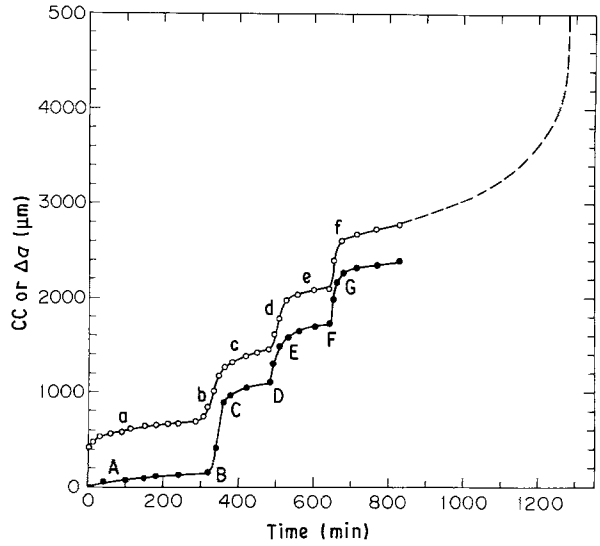

Figure 3 (○) Notch opening, CC, and (●) crack advance, Δa, as function of loading time. Specimen was loaded at 80 °C and 2.4 MPa. Complete failure in 1276 min.

relationship between Figs 3, 4 and 5 will now be explained.

The structure in the slow interval designated by "a" in Fig. 3 is represented by Figs 4a and 5a. The structure is essentially a craze. Fig. 5b shows that fracture initiates within the craze leaving a strong film at the root of the notch. The initiation of fracture is represented by points b and B in Fig. 3. Fig. 4b shows both the unbroken film at the root of the notch and the adjacent fibrillated region which is just beginning to fracture.

Fig. 5c shows that the first strong film has fractured and the crack has advanced. Detailed observations showed that the jump from b to c and from B to C in Fig. 3 occurred when the crack advanced rapidly ahead of the first strong film and then the first strong film began to fracture as shown in Figs 4c and 5c. Thus, the strong film fractures shortly after the crack has advanced rapidly within the craze.

The crack then stops, and a second strong film forms at the bottom of the crack with the fibrillated structure of the craze behind it. Now the second slow interval from C to D in Fig. 3 occurs. During this slow interval a subsidiary damage zone occurs at about 45° to the main crack and at the point where the second strong film forms. The position of the strong film is marked by the subsidiary damage zones at 45° and by a long and thick broken fibril at the fractured surface.

The fracture process repeats itself as follows. (1) There is the slow interval where the craze grows slowly while a strong film forms at its base. (2) Fracture initiates behind it and jumps ahead and shortly thereafter the front strong film fractures.

Fig. 8d (see later) is a top view of the completely fractured surface which corroborates the above description of the fracture process. In Fig. 8d, AB is the first strong film. BC is the interval of rapid advance prior to complete fracture of the film at AB. CD is the point of crack arrest where the second strong film forms. The fracture surface in Fig. 8d corresponds to the side view of the same specimen in Fig. 5g, and

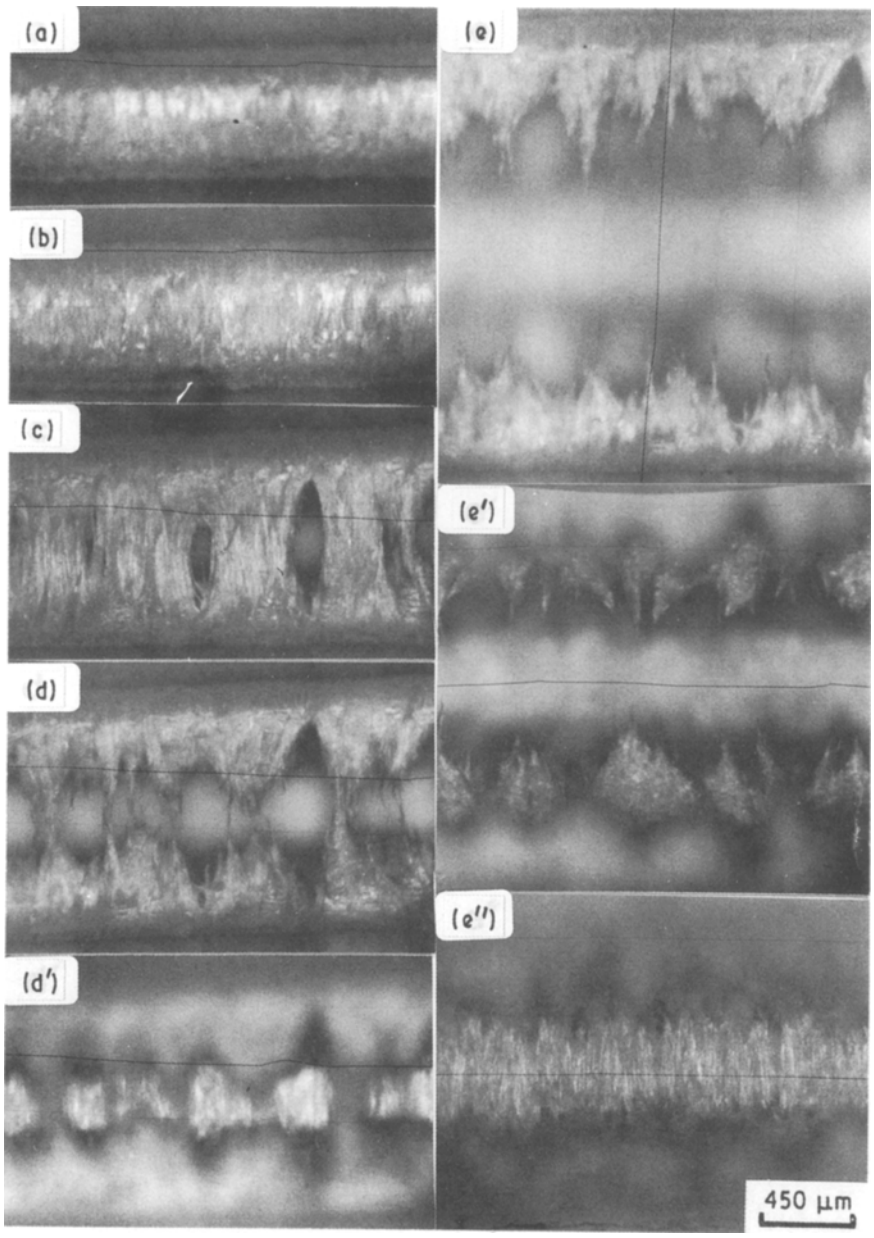

Figure 4 Views into root of notch at different times with optical microscope. (a) to (e) correspond to times designated (a) to (e) in Fig. 3. (d) and (d') are at the same time but the focus in (d) is the first crack arrest and (d') at the second arrest. At a later time, (e), (e') and (e'') are focused on the first, second and third points of arrest, respectively.

both of these figures correspond to the specimen whose kinetic behaviour is shown in Fig. 3. Figs 5g and 8d show that there were three crack arrests before the final very rapid and unstable fracture process.

Fig. 6 shows more details of the fracture process. The optical transmission micrograph, Fig. 6a, shows that the primary craze ahead of the crack is dark and that the subsidiary damage zones at about 45° are also dark. However, in reflected light, Fig. 6b, these dark regions are bright. This change in contrast from dark to light in transmitted and reflected light, respectively, is expected for a porous structure. This behaviour is characteristic of a craze. It is also evident that the damage zone where fracture initiates is a craze as indicated by its fibrilla structure. It is also evident that the subsidiary zone at 45 °C is not simply a zone of shear with the same density as the matrix; its contrast behaviour indicates that it contains appreciable porosity. Probably the subsidiary deformation zone is a combination of a shear band and a craze whose fibrilla structure is not discernible with the microscopic techniques that were used.

The formation of the subsidiary deformation zone relaxes the stress on the boundary of the newly formed primary damage zone and therefore delays the initiation of fracture.

The strong film at the point of arrest does not exhibit the contrast that is characteristic of the porous region associated with the primary craze. Its contrasting behaviour indicates that its density is close to that of the matrix. The film appears to behave like a tensile specimen formed under plane stress conditions so that it undergoes shear without the formation of appreciable voids.

3.3. Stress dependence of discontinuous slow crack growth

Fig. 7 shows variation of the notch opening with time at various stresses. For stresses at 3.2 MPa and below, failure is by slow crack growth and it is called brittle failure. Above 3.2 MPa the failure mode undergoes a transition to ductile failure and above 3.9 MPa the failure is purely ductile. The slow crack growth is

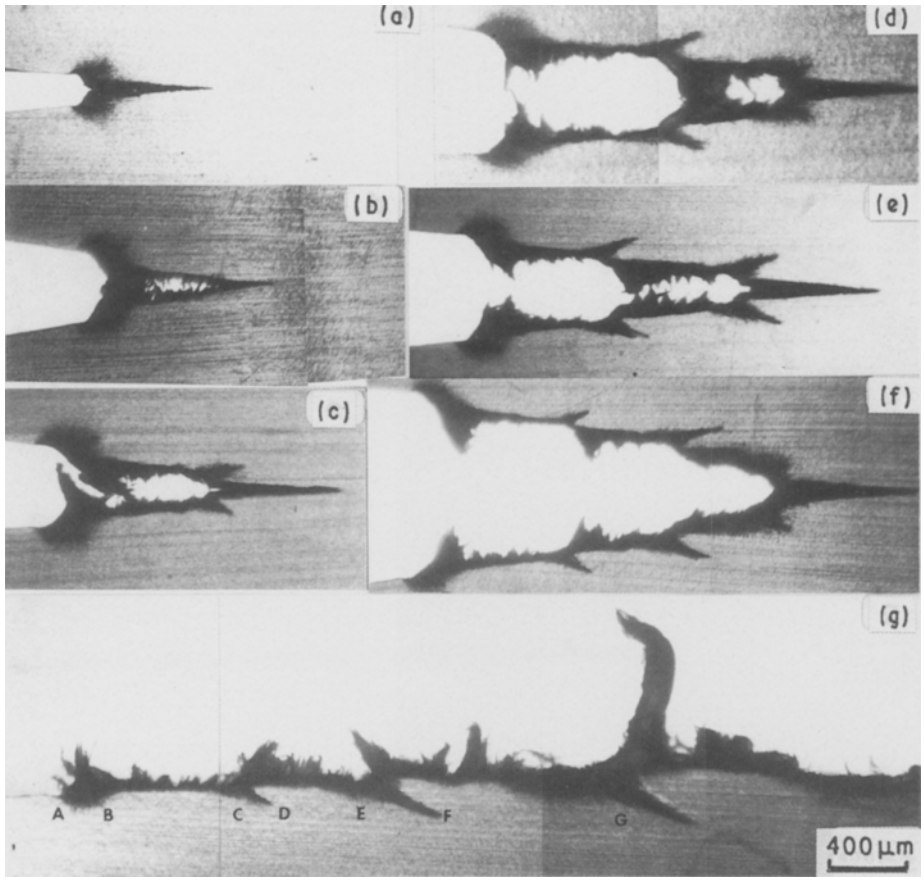

Figure 5 Side view of notch as viewed with optical transmission microscope of a series of specimens loaded for different times (a) to (f) which corresponds to times designated (a) to (f) in Fig. 3.

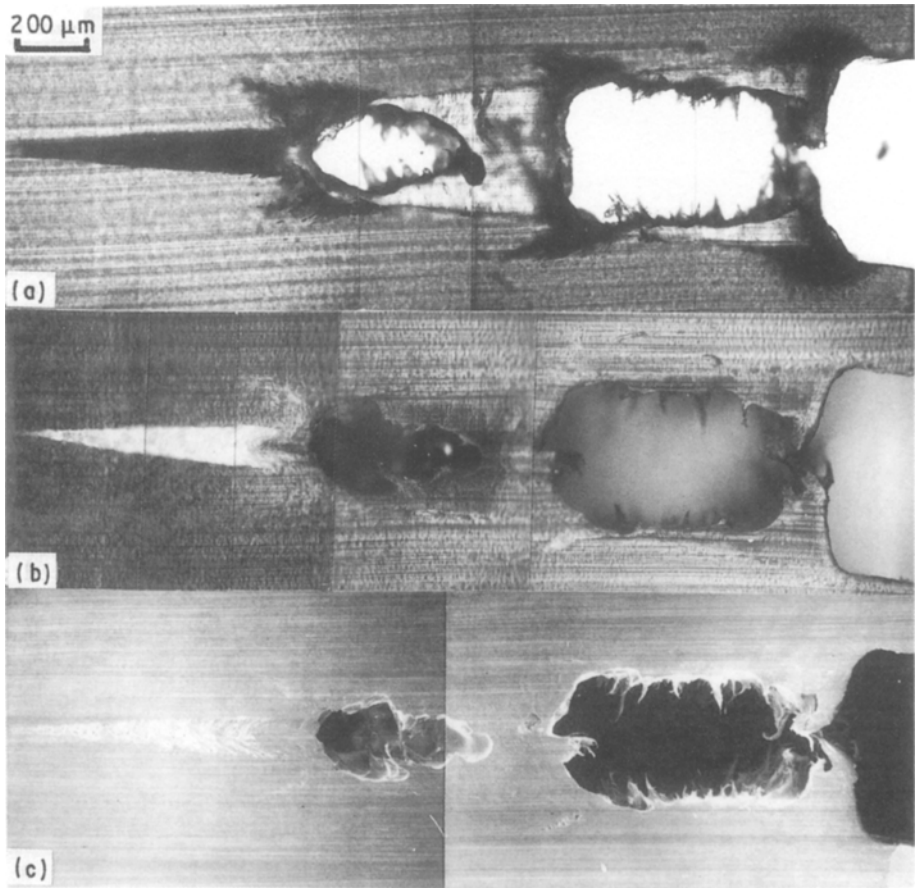

Figure 6 Micrographs of damage zone in specimen loaded at 80 °C, 2.4 MPa for 500 min. (a) Optical transmission; (b) optical reflection; and (c) scanning electron micrograph.

observed to be discontinuous down to a stress of 1.2 MPa as observed by the change in COD with time. The number of arrests increases as the stress is reduced, while the magnitude of the jump in COD decreases. For stresses below 1.2 MPa, jumps in the COD–time curve could not be observed.

The morphology of the fractured surfaces are shown in Figs 8 and 9 for stresses in the brittle region. The

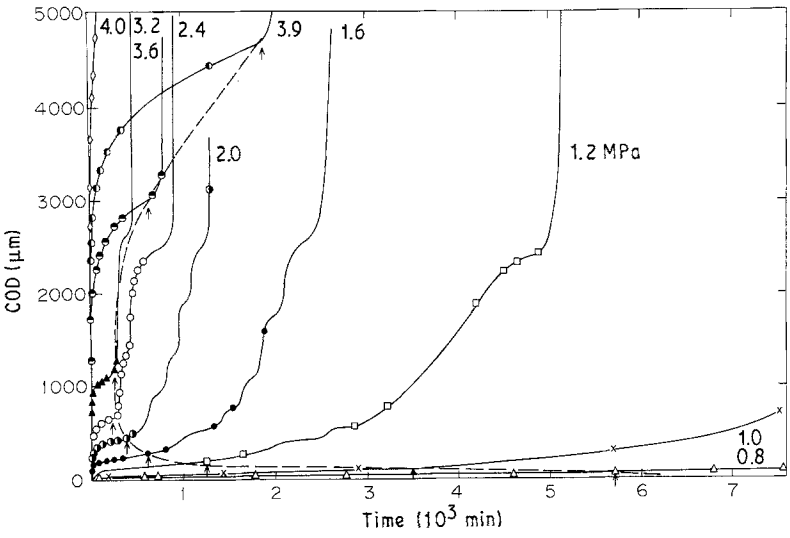

Figure 7 Notch opening, CC, plotted against time at 80 °C for various stresses. Arrows indicate when fracture initiated.

Figure 8 Fractured surface of specimens tested at 80 °C at different stresses: (a) 1.2 MPa, (b) 1.6 MPa, (c) 2.0 MPa, (d) 2.4 MPa, (e) 2.8 MPa, (f) 3.2 MPa. See text for explanation of letters in Fig. 8d. Original notch at bottom of figures.

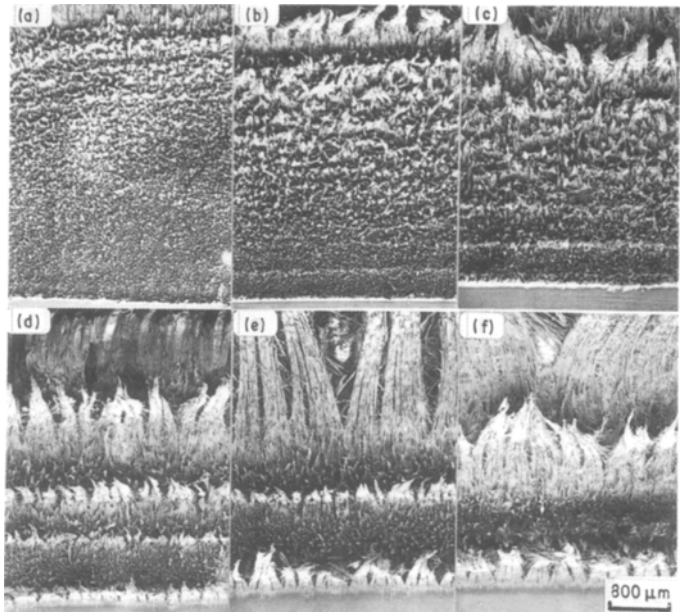

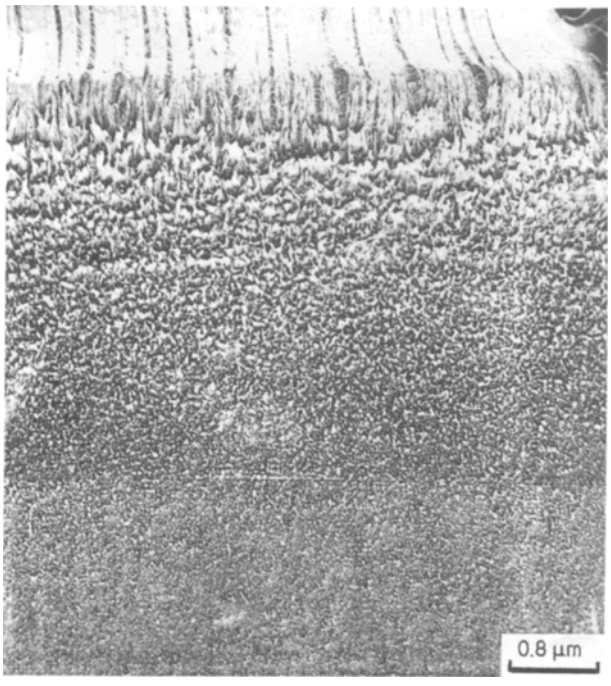

Figure 9 Same as Fig. 8 for 1.0 MPa. Crack arrest lines are only visible at the end of the fracture process.

spacing of the crack arrests increases with increasing stress which agrees with the curves in Fig. 7. The height of the fibrils increases with stress. The spacing of the arrest lines increases with each advance as does the height of the fibrils. These results are in agreement with Fig. 5 where the height of the fibrils corresponds to the dark zone on the border of the crack.

Whereas discontinuous crack growth could not be observed in Fig. 7 for a stress below 1.2 MPa, Fig. 9 shows arrest lines at 1.0 MPa.

Fig. 10 contains a plot of the average spacing, $\bar{d}$, of the arrest lines against σ^2. The relationship is represented by

$$\bar{d} = 127\,\sigma^2(\mu\text{m, MPa}) \qquad (1)$$

The data indicate that $\bar{d}$ approaches zero when σ approaches zero. This result suggests that discontinuous crack growth occurs down to the lowest stress level, and that the jumps in COD become too small and too closely spaced to be measured by our measuring technique for stresses less than 1.2 MPa. Also, at very low stresses, the arrest lines are not always visible by our microscopic method. When the

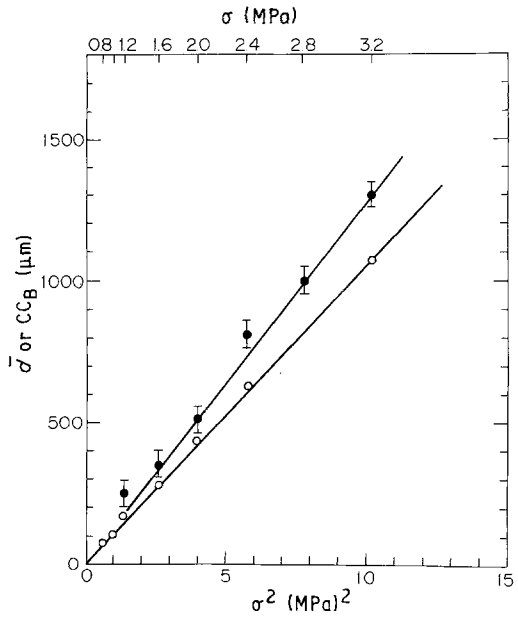

Figure 10 $\bar{d}$, (●) Average spacing of arrest lines from Fig. 8 and (○), the notch opening of fracture initiation plotted against the square of the stress at 80 °C.

arrest lines are very finely spaced, the intrinsic size of the fibrils tends to obscure them.

In Fig. 10 the notch opening displacement, CC, at the time that fracture was initiated is plotted against σ^2. The linear relationship is

$$\text{COD(at fracture initiation)} = 105\,\sigma^2(\mu\text{m, MPa}) \quad (2)$$

This result is in agreement with the Dugdale theory. The height of the fibrils that are observed in Fig. 8 closest to the notch tip correspond to about half of the COD that occurs at the initiation of fracture.

3.4. The temperature dependence of slow crack growth

The morphologies of the fractured surfaces for temperatures from 42 to 80 °C are shown in Fig. 11 for 2.4 MPa. The spacing of the arrest lines and the height of the fibrils increase with increasing temperature. These results agree with COD–time curves at various temperatures. The average spacing of the arrest lines and the COD at crack initiation were plotted with respect to σ_y^2, where σ_y is the yield point at the corresponding temperature. The results are

$$\bar{d} = 240 + 3.0 \times \frac{10^4}{\sigma_y^2}(\mu\text{m, MPa}) \quad (3)$$

and

$$\text{COD (at crack initiation)} = 100 + 2.5\left(\frac{10^4}{\sigma_y^2}\right)(\mu\text{m, MPa}) \quad (4)$$

4. Discussion

The experimental observations produced the following picture of discontinuous slow crack growth.

1. A craze is formed of length Δa as soon as the specimen is loaded where according to the Dugdale

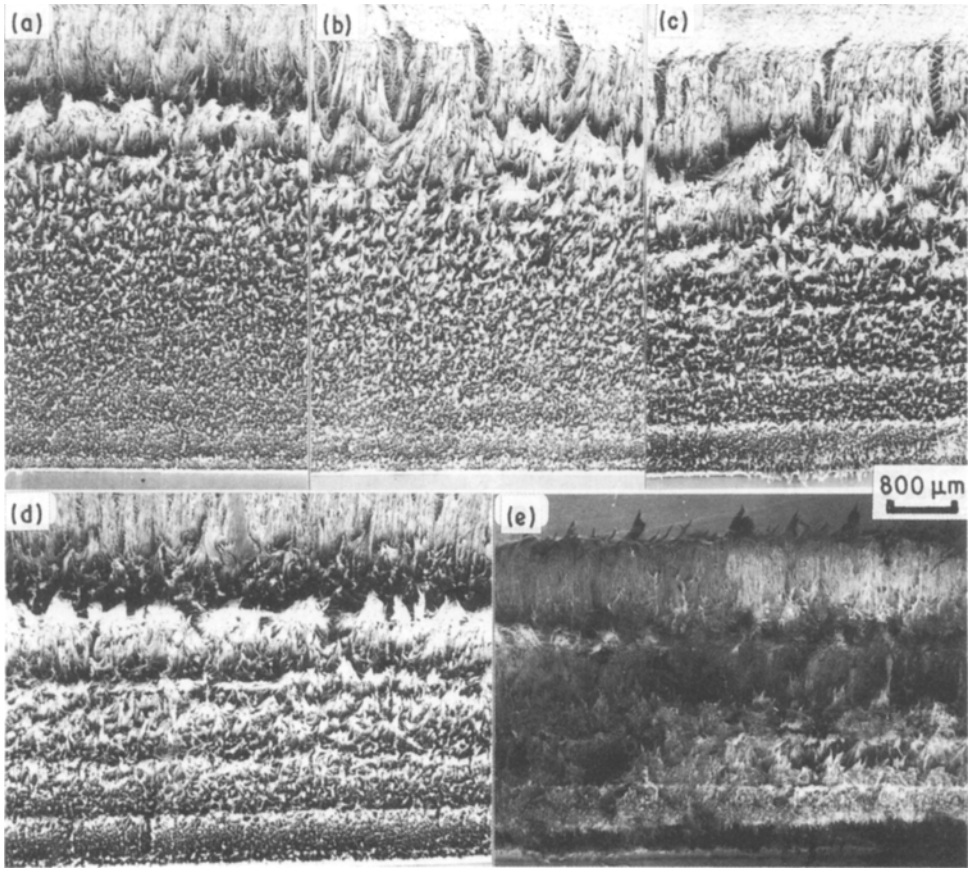

Figure 11 Fractured surface of specimens tested at 2.4 MPa at different temperatures: (a) 42 °C, (b) 50 °C, (c) 60 °C, (d) 70 °C and (e) 80 °C.

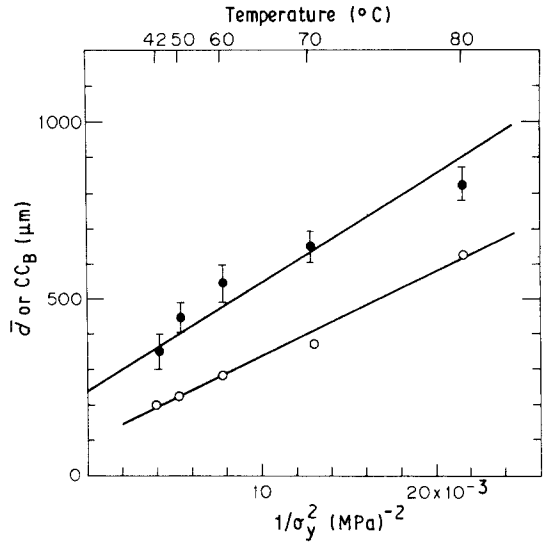

Figure 12 (●) Average spacing of arrest lines from Fig. 11, $\bar{d}$ and (○) notch opening at cracking initiation plotted against $1/\sigma_y^2$ where σ_y is yield point at the different temperatures. The applied stress was constant at 2.4 MPa.

theory

$$\Delta a = \frac{\pi}{8}\frac{K^2}{\sigma_y^2} \quad (5)$$

2. The craze length and the craze opening displacement increase slowly.

3. The base of the craze consists of a strong continuous film instead of the fibrillated structure that occurs within the craze.

4. Subsidiary damage zones occur at the base of the craze and make an angle of about 45°.

5. Fracture initiates in the fibrilla region at the base of the craze next to the strong film.

6. The crack grows quickly to a distance about two-thirds of the length of the craze and then stops.

7. During the rapid advance of the crack, the notch opening displacement also increases rapidly and the crazed region in front of the crack also increases rapidly.

8. Shortly after crack initiation, the strong film at the base of the craze fractures.

9. The process is repeated in that the craze now grows slowly and another strong continuous film with the subsidiary damaged zones at 45° forms again.

10. When the crack grows it advances a greater distance before stopping than during its previous advance.

The distance between arrest lines increases with each successive jump and also increases with the applied stress and with increasing temperature. This behaviour is simply explained by the fact that the larger the craze the larger the possible distance that the crack can advance rapidly. The size of the craze is simply based on the Dugdale equation as given by the above equation.

The more interesting questions are (1) why the crack is arrested, (2) why a strong continuous film forms at the root of the crack and, (3) the role of the subsidiary zones of damage at 45°.

When the crack is initiated, the stress intensity increases so that the driving force for crack growth increases as the crack advances. The reason that the crack stops is because the fibrils in the craze increase in strength in going from the base of the craze to its tip. When the craze first forms, the fibrils are extended by different amounts with the fibrils at the base being closest to δ_c, the critical craze opening for fracture. Thus, the crack stops at the point where the fibril is too strong to be broken at that moment by the prevailing stress intensity. The time for crack initiation depends on the rate of disentanglement of the molecules within the fibril. This disentangling rate is fundamentally responsible for overall speed of the crack growth process.

The strong film that forms at the base of the craze and which fractures after the crack initiates within the adjacent fibrils is a special part of the craze. It forms under the plane stress conditions at the root of the crack. It is stronger than the fibrils because it is not shredded by the large hydrostatic component of the stress which acts on the inner part of the craze.

The subsidiary side bands form when the crack is arrested and they are produced mainly by the shear component of the stress field that occurs at the corners of the crack at its bottom. These side bands are not pure shear zones in that they are somewhat porous. The side bands and the craze itself grows during the period of crack arrest because the yield point of the polyethylene decreases with time. The subsidiary damage zone also tends to prolong the time of crack arrest by relaxing the local stress concentration on the fibrils. This relaxation effect has been observed in crystalline solids where the stress which tends to produce fracture is reduced by shear bands at 45° to the plane of fracture.

Thus, crack arrest is basically caused by the fact that the advancing crack runs into fibrils that are too strong to be broken at that instant of time. The crack then initiates after the slow process of disentanglement sufficiently weakens the fibrils.

In homopolymers with low molecular weight, the disentangling process is very rapid. Thus, the time between crack arrests becomes very short so that discontinuous crack growth has not been observed by our experimental technique. In general, discontinuous crack growth is considered to be a general process but it may not be observed if the distance of rapid crack advance is too small and/or if the rate of disentanglement of the fibrils is too fast.

5. Conclusions

1. The geometric features of discontinuous crack growth such as the spacing of the arrest lines and the height of the fibrilla structure as they depend on stress and temperature, are all explainable within the framework of the Dugdale theory. The distance of rapid crack advance is directly related to the size of the craze which increases with the parameter K^2/σ_y^2.

2. The time for crack initiation depends on the rate at which the fibrils weaken by a process of disentanglement.

3. The advancing crack stops because the strength of the fibrils continuously increases in going from the base of the craze toward its tip.

4. The base of the craze consists of a thin, strong continuous film because it forms under plane stress conditions.

5. Discontinuous crack growth is a general phenomenon but tends to become unobservable as K^2/σ_y^2 decreases and/or as the rate of disentanglement increases.

Acknowledgements

The work was supported by the Gas Research Insititute and the Department of Energy. The Central Facilities in the Laboratory Research on the Structure of Matter as supported by NSF were most helpful.

References

1. R. W. HERTZBERG and J. A. MANSON, "Fatigue of Engineering Plastics" (Academic Press, New York, 1980) p. 160.
2. M. K. V. CHAN and J. G. WILLIAMS, *Polymer* **24** (1983) 234.
3. A. LUSTIGER and R.D. CORNELIUSSEN, *J. Mater. Sci.* **22** (1987) 2047.
4. N. BROWN and X. LU, "The Kinetics and Microscopic Processes of Long Term Fracture in Polyethylene Piping Materials", GRI-88/0135 Report, Gas Research Institute, 8600 West Bryn Mawr Ave., Chicago, Illinois 60631, USA.
5. A.W. HESTON, MS thesis, Department of Mech. Eng. and Appl. Med., University of Pennsylvania (1983).

Received 22 February
and accepted 9 March 1990